Feature Recognition Using Volume Data with Application Spinal Fracture Diagnosis

Ming-Dar Tsai[1*], Yi-Der Yeh[1], Ming-Shium Hsieh[2]

[1*]Ming-Dar Tsai Associate Professor, contact author
Institute of Information and Computer Engineering, Chung Yuan Christian University
ADDRESS: Chung Li, 32023 Taiwan, R.O.C.
TEL: (+886) 3-256-4718 FAX: (+886) 3-256-4799 E-MAIL: tsai@ ice.cycu.edu.tw

[1] Yi-Der Yeh Doctoral student,
TEL: (+886) 3-256-4715 FAX: (+886) 3-256-4799 E-MAIL: yeh@earth.ice.cycu.edu.tw

[2] Ming-Shium Hsieh Associate Professor and Chairman,
Department of Orthopaedics and Traumatology, Taipei Medical University Hospital, Taipei Medical University,
ADDRESS: 252, Wu Hsing Street, 11031 Taipei, Taiwan, R.O.C
TEL: (+886) 2-2737-2181(3118) FAX: (+886) 2-2737-5618 E-MAIL: shiemin@tmu.edu.tw

Abstract

This paper describes feature recognition methods for the evaluation of 3D geometry of vertebral bones and spinal anatomic curve in the diagnosis of compression and burst fractures. The method uses a radial B-spline curve to extract the feature of the ellipse-like vertebral body on a transverse section in which a concave feature is also recognized to evaluate the compression of the canal. 3D feature of infers the anatomic curve of a vertebral body is recognized by linearly regressing the centers of B-spline approximate ellipse-like boundaries of the transversal sections passing the vertebral body. Then, the reduced angle and height for recovering the compression fracture can be calculated by comparing the regressed centerlines of neighboring bodies of the fracture body with the normal spinal anatomic curve. The prototype system can be used as a qualitative and quantitative tool for the diagnosis of compression and burst fractures using transverse sections, and for the instruction to plan accurate surgical procedures.

Keywords: Feature recognition, Image analysis, B-spline radial approximation, 3D image reconstruction, medical application, spinal fracture

1. Introduction

Feature recognition has been applied to traditional (B-rep: boundary representation or CSG: constructive solid geometry) solid models for extracting geometric properties of a solid, that can be used in a CAD or CAM system for automatic designing or manufacturing a product in various industries (e.g. [1]). A feature, in a B-rep or CSG model, is recognized based on the results of intersection computation between original boundary edges and the lines connecting vertices [2-4]. However, such application is seldom available to a volume model because a volume does not record any boundary face or edge. Although isosurface reconstruction techniques can obtain even millions of triangles from a medical volume to render 3D realistic images for visualization, these triangles are actually a surface model cannot automatic geometric characters about solids in the volume.

Some approach did not use the 3D way to search features in a medical volume but search 2D features in respective sections (that constitute the volume) then to reconstruct 3D features by the 2D features. For example, ellipse-like intervertebral disc boundary can be also well approximated as a B-spline radial and closed curve associated with concave and convex features. The convex features are then matched into a disc herniation feature then used to diagnose HIVD [5]. The 2D features of consecutive sections also infer a 3D feature indicating the 3D geometry and location of the herniation that is useful to assist planning surgical procedures. This study extends such feature recognition way to recognize more 2D and 3D features. These 3D geometric properties are applied to a tool for diagnosing spinal fractures.

Patients with spinal fractures are not accurately diagnosed on clinical findings because an exact diagnosis of a spinal fracture must analyze the 3D geometry of compressed vertebral bones and burst bone fragments and the relations between the compressed bones with the spinal cord and their neighboring vertebral bones [6-8]. The diagnosis of a vertebral fracture must determine the degree of the fracture. Two kinds of compressed degrees must be evaluated: the deformation of anatomic curve and the reduction of the canal. These degrees determine the surgical modalities and procedures for the correction or reduction or decompression of the compressed bones and the spinal cord [9,10]. For example, the frequently applied instrumentation with posterior lateral pedicle screw (either for compression or distraction purposes) must use the information of deformed curve and reduction area of the canal to decide distracted disc and vertebral distances, and recovery spinal angles [11,12]. This paper proposes a method to determine the degree of a vertebral fracture by recognizing the shape feature of the compressed bone and its neighboring bones. In this preliminary

study, we evaluated the usefulness of our method by a medical volume of a fractured patient.

2 A Vertebral Body Model

Fig. 1(A) shows a fractured vertebral body in which the anterior height became smaller to form an axis deformation of the vertebral bones (as shown in Fig. 1(B)). The fractured vertebral body may be sheared to form axis deviation. Some fragments of the fractured vertebral body may burst into the canal to reduce its diameter (Fig. 1(A)). The boundary of a vertebral body on a transverse (even little oblique) section can be considered as ellipse-like with a concave feature that forms the canal. If the transverse section (as Section *A* in Fig. 1(B)) passes the upper of the vertebral body, the concave feature of the vertebral body and the bilateral pedicle and lamina form a closed bone boundary at the canal. However, the boundary is not closed if the transverse section does not pass the pedicle and lamina (as Section *B* in Fig. 1(B)).

A vertebral body on a transverse section can be approximated by a B-spline curve that has good approximation for circle, arc, sine or cosine- like boundaries [13,14]. This study also approximates the boundary of a vertebral body on a transverse section as a B-spline radial and closed curve associated with a concave feature enclosing the canal. The canal has the smallest diameter along the anteroposterior direction. Moreover, a canal has a large probability invaded by burst fragments of a vertebral body and pedicle during the vertebral fracture that mainly reduce the diameter along the anteroposterior direction. Therefore, a canal reduction during the vertebral fracture can be evaluated by the reduction of the diameter along the anteroposterior direction. The compressed diameters of the canal on the sections of the fractured vertebral bone and the normal diameters on the sections of its neighbors can be compared to decide the compressed ratio of the canal.

Multiple transverse sections may pass the same vertebral bone to obtain different compressed ratio. The severest one is used to determine the degree of the fracture. The multiple sections also determine a centerline of the vertebral body. The angle between the centerlines of the above and below neighboring vertebral bodies to the fractured body can be used to compare with the normal anatomic angle between the center axis of the above and below neighboring vertebral bodies to determine the angle reduction for recovering the angle deformation. This heights of centerlines of neighboring bodies are used to determine a normal height of the fractured body to compare its fractured height, thus to determine the distracted or compressed distance.

3 2D Feature Recognition of Vertebral Body for Determination of Body Center and Canal Diameter Calculation on a Transverse Section

The process of matching a vertebral body boundary and canal diameter along the anteroposterior axis on a transverse section is described as follows.

1. Determine the center of bone tissues on a transverse section by averaging the position of the pixels of bone tissues (Fig. 2(A)). Because the area of the vertebral body on a transverse section is larger than the sum of pedicle and lamina, the center is located inside the vertebral body. A transverse section may pass a disc space in which disc substances and bone tissues coexist inside the ellipse-like boundary. For such transverse section, the pixels of disc substances are also used together with the ones of bone tissues to determine the center.
2. Use a vector starting from the center along every (totally 360) integral angular position to intersect the bone boundary. If multiple intersections were obtained, cracks or a hole exist inside the bone tissues. If the distance of two consecutive intersections of the same angular position is small, it is a crack that appears after the fracture and usually occurs at the vertebral body and pedicle. If the distance of two consecutive intersections is large and a number of neighboring angular positions have such pairs of intersections, it is the canal boundary. When calculating the center of vertebral body, the crack intersections are ignored. From the center to lamina, pedicle and transverse process, multiple intersections (except the ones intersecting the cracks) are obtained. The left pedicle, lamina and transverse process can be excluded from the body using the boundary interpolated from the radius $r_s(L)$ of the leftmost angular position of the canal with the radius $r_s(Ln)$ of the angular position without multiple intersections (as shown in Fig. 2(A)), meaning that the radius of an angular position in-between the two angular positions is linearly interpolated by $r_s(L)$ and $r_s(Ln)$. Similarly, the right pedicle, lamina and transverse process can be excluded from the body by the boundary interpolated from the radius $r_s(R)$ of the rightmost angular position of the canal with the radius $r_s(Rn)$ of the angular position without multiple intersections.
3. Determine the center of vertebral body by averaging the boundary pixels (already excluding the cracks, pedicle, lamina and transverse process) at the 360 angular positions (Fig. 2(B)), then repeat the above step to determine the radius of every angular position, e.g., the radii ($r(L)$ and $r(R)$) from the center to the leftmost and rightmost angular

position of the canal. Then, we use the new radii of the 360 boundary pixels to approximate a B-spline curve for the vertebral body [15].

4. Determine the middle point *C* on the boundary of the canal. Its angular position to the center of the vertebral body is the average of the leftmost and rightmost angular positions of the concave feature enclosing the canal, and its radius can be calculated using the B-spline curve (as shown in Fig. 2(B)).
5. Determine the anteroposterior diameter *CD* following the location of the opposite point (*D*) of *C*. Use vectors starting from *C* across the canal boundary (first intersection) to intersect other bone boundaries. A range of intersections with large distances are considered intersecting with the spinal process. The average vector of the leftmost and rightmost vectors of the range intersects *D* (Fig. 2 (C)). If the spinal process is not resolved in the transverse section. Then, the spinal space is used to locate *D*. We use vectors starting from *C* across the canal to intersect the air. A range of intersections that intersected the spinal space can be obtained (Fig. 2 (D)). Then, the average vector of the leftmost and rightmost vectors of the range intersects *D* (Fig. 2 (D)). If this section resolves no spinal process and space, the vectors stating from *C* to opposite boundary of the canal are approximated as a quadric radial function. The vector that is the local maximum of the function intersects *D* (Fig. 2 (E)).

4 3D Feature Recognition for Determination of Compression Ratio and Recovering Angle and Distance Calculation from Transverse Sections

The anteroposterior diameter calculation method, described in the last section, determines the diameter on each section. Because the diameters of transverse sections in a normal vertebral bone should be near the same, the average of the diameters of all the transverse sections can represent the canal diameter in this vertebral bone. However, if some diameter has large deviation to the average, it is abandoned, and the average is re-determined. The normal (before fracture) diameter of the fractured vertebral bone is then, interpolated or extrapolated from neighboring bones of the fractured bone. The compression ratio on any transverse section of the fractured bone is the ratio of the anteroposterior diameter on the section to the interpolated or extrapolated normal value. The worst (smallest) ratio is used to represent as the compression ratio by the fracture.

We compute the angle and distracted or compressed distance for recovering using the centers calculated in all

transverse sections as the following procedures.

1. Determine a centerline for each vertebral body that regress the centers of the transverse sections passing this body with least square errors [16]. The two ends of the line are located on the middles of the above and below neighboring disc spaces. However, if there exists some center with large deviation, the center is neglected and the line is re-determined (Fig. 3(A)). However, if the distance between the centers of two neighboring sections is too large, a shear dislocation is considered existing inside the fractured vertebral bone (Fig. 3(B)). Then, two respective centerlines are used to regress the two dislocated parts of the body. Then, the distance between the two lines is considered the shear dislocation by the fracture.
2. Determine the compressed angle by the centerlines of above and below neighboring vertebral bodies of the fractured body. α represents the angle of the two lines after the fracture (Fig. 3(D)) and β represents the angle of the two lines if no fracture (Fig. 3(E)) that follows the normal anatomic (first or secondary) curve [17].
3. Determine the distracted or compressed distance. The length of a centerline represent the height of a vertebral body, while the normal height (before the fracture) of the fractured body can be interpolated or extrapolated by the lengths of neighboring vertebral bodies (without the fracture). Then, the distracted or compressed distance is the difference of the interpolated normal height with the height (length of the centerline) of the current fractured body.

5. Implementation

Currently, the system is implemented on a P-IV 1.4G PC. A patient with a typical fractured spine was used to demonstrate the results implemented by our system. He was a 39-year-old man and suffered from a falling-down from six-meter height. Clinical findings were indicative of spinal cord lesion below L2. CT was performed in 48 transverse sections (256×256 resolutions) from L3 (the third lumbar spinal bone) to T11 with all 7 degrees oblique to the transversal plane and constant 3mm intervals. These sections were taken to be perpendicular to L2. Fig. 4 shows a section from L1 a normal vertebral bone demonstrating no canal compression and fracture, and a section from L2 demonstrating the canal compression and fracture. Fig. 5 shows 3D images that rendered the isosurfaces reconstructed from the marching cube algorithm. Fig. 5(A) shows the lateral view that demonstrates a serious compression on L2, especially the anterior column that brings kyphosis. Fig. 5(B) shows the frontal view that also demonstrates the un-symmetric horizontal compression on

L2 that brings scoliosis. Fig. 5(C) shows the posterior view that demonstrates the positions for inserting posterior lateral pedicle screws for fracture reduction and posterior fusion. Fig. 5(D) shows the images of the recognized (B-spline approximate) vertebral bodies wherein the pedicle, lamina, transverse and spinal process were excluded. Therefore, the bone fragment (with a crack as shown in Fig. 4(B)) burst into the canal at L2 can be easily observed.

Fig. 6(A) shows a simplified 3D image revealing the relations between the vertebral bodies in which the thickness of a cylinder is the height of a vertebral body, the axis direction of the cylinder is the direction of the centerline and the radius of the cylinder is the average radius of the B-spline approximate body. By comparing Fig. 6(A) with Fig. 5(A) wherein the body centerline directions and heights are similar, the centerlines of the bodies were correctly calculated can be observed. Fig. 6(D) shows a simplified 3D image in which the cylinder of L2 uses the assumed normal (before the fracture) centerline (direction and height) not the calculated fractures centerlines. Fig. 6(C) and Fig. 6(D) and Fig. 6(E) show the results of morphing from Fig. 6(A) until Fig. 6(D). Such information is useful in demonstrating whether the recovery from the spinal reduction is acceptable. The operation based on the calculated reduced angle and height was implemented. The above clinical syndrome disappears immediately after the surgery, and lateral and anteroposterior X-rays show good immediate reduction of bones.

6. Conclusion and Future Work

In this study, we developed a diagnostic method that can automatic determine the compression ratio, the reduction angle and height for recovering the fractured bone. The 3D characteristic of the fractured bone, the bone fragment bursting into the canal, the relation between the fractured bone with neighboring bones and the spinal cord, and the angle and height for recovering can be clearly revealed. Using this tool, clinicians can quantitatively and accurately, with a spatial concept, evaluate conservative or surgical modalities and procedures for fractured bones. A clinical example was diagnosed using the prototype system to demonstrate that the compression and shear dislocation of the vertebral body, the burst fragment to the canal, and the reduced height and angle can be accurately evaluated.

Our method uses a B-spline curve to approximate the vertebral body boundary and a concave feature enclosing the canal on a transverse section, thus to determine the center of a vertebral body and the diameter and the compression ration of the canal. Then, our method uses centerlines to regress the centers of transversal sections. The deformed height and

angle of the fractured bone can be estimated by the centerlines of the fractured bones and its neighboring bones, so that to determine the reduction height and angle for recovering the fracture. These estimations can be demonstrated in 3D images using any commercial CAD or graphics software.

Our method can represent realistic 3D images using our volume visualization software. Our volume visualization and surgical simulation software can render isosurfaces reconstructed from volumes and simulate musculoskeletal surgeries [18-20]. However, because of the inheritance of volume structure, our method can only translate anatomic structures but cannot rotate structures. Therefore, we use commercial graphic software to simplify the recovering results by the decompression and fusion surgery. This is our future works that extend the surgical simulation software to simulate the decompression and fusion surgery so that realistic 3Dimages can be used to demonstrated the procedures and results of the decompression and fusion surgery.

Acknowledgment

This study was partially sponsored by the National Science Council (NSC), Taiwan/ROC; grant numbers NSC-91-2213-E-033-024 and NSC-91-2314-B-038-034.

Reference

1. Fu M.W., Fuh J.Y.H., Nee A.Y.C. Undercut feature recognition in an injection module design system. Computer-Aided Design 1999; 31: 777-90.
2. Li C.L., Hui Y.S. Feature recognition by template matching. Computer and Graphics 2000; 24: 569-82.
3. Xu X., Hindujia S. Recognition of rough machining features in 2D components. Computer-Aided Design 1998; 30: 503-16.
4. Sakurai, H, Gossard, D.C. Recognizing Shape Features in Solid Models. IEEE Computer Graphics and Applications, 1990; 10: 22-32.
5. Tsai MD, Hsieh MS and Jou SB: A New Method for Lumbar Herniated Inter-Vertebral Disc Diagnosis based on Image Analysis of Transverse Sections. Comput Med Imag Grap. Page proof completed.
6. Van Beek EJR, Been HD, Ponsen KJ and Mass M: Upper thoracic spinal fractures in trauma patients – a diagnostic pitfall. Injury, Int. J. Care Injured 2000; 31: 219-223.

7. Hu RW: Orthopaedic Knowledge Update, Trauma 2. In: Kellam JF, Fischer TJ, Tornetta III P, Bosse MJ, Harris MB, editors. Evaluation and assessment of the polytrauma patient for spinal injuries, Rosemont: American Academy of Orthopaedic Surgeons 2000; 319-328.

8. Wood KB: Orthopaedic knowledge update, Trauma 2. In: Kellam JF, Fischer TJ, Tornetta III P, Bosse MJ, Harris MB, editors. Thoracic spine injuries, Rosemont: American Academy of Orthopaedic Surgeons 2000; 371-381.

9. Hitchon PW, Torner JC, Haddad SF and Follett KA: Management options in thoracolumbar burst fractures. Surg Neurol 1998; 49: 619-626.

10. Esses SI, Botsford DJ, Wright T, Bednar D and Bailey S: Operative treatment of spinal fractures with the AO internal fixator. Spine 1991; 16: 146-150.

11. Andress HJ, Braun H, Helmberger T, Schürmann, Hertlein H and Hartl WH: Long-term results after posterior fixation of thoraco-lumbar burst fractures. Injury, Int. J. Care Injured 2002; 33: 357-365.

12. Theodorou DJ, Theodorou SJ, Duncan TD, Garfin SR and Wong WH: Percutaneous balloon kyphoplasty for the correction of spinal deformity in painful vertebral body compression fractures. Clinical Imaging 2002; 26: 1-5.

13. Panda B and Chatteji BN: Least square generalized B-spline signal and image processing. Signal Processing 2001; 81: 2005-17.

14. Chuang SHF and Kuo CZ: One-sided arc approximation of B-spline curves for interference-free offsetting. Computer-Aided Design 1999; 31: 111-18.

15. Burger P and Gillies, D: In: Interactive Computer Graphics, Cubic B-spline. Addison Wesley company, New York 1989. p. 250-264.

16. Cheney W and Kincaid D: Smoothing of data and the method of least squares. In: Numerical Mathematics and Computing, Brooks/Cole(Eds.), 1994, ch.10: 381-409.

17. Bridwell and DeWald: The textbook of spinal surgery. Philadelphia: Lippincott JB 1996, 570.

18. Tsai MD, Jou SB and Hsieh MS: Accurate Surface Voxelization for Manipulating Volumetric Surfaces and Solids with Application in Simulating Musculoskeletal Surgery. Pacific Graphics. 2001; IEEE CS press: 234-43.

19. Tsai MD, Hsieh MS and Jou SB: Virtual Reality Orthopedic Surgery Simulator. Comput Biol Med. 2001; 31(3): 333-351.

20. Hsieh MS, Tsai MD and Chung WC: Virtual Reality Simulator for Osteotomy and Fusion Involving the Musculoskeletal System, Comput Med Imag Grap. 2002; 26(2): 91-101.

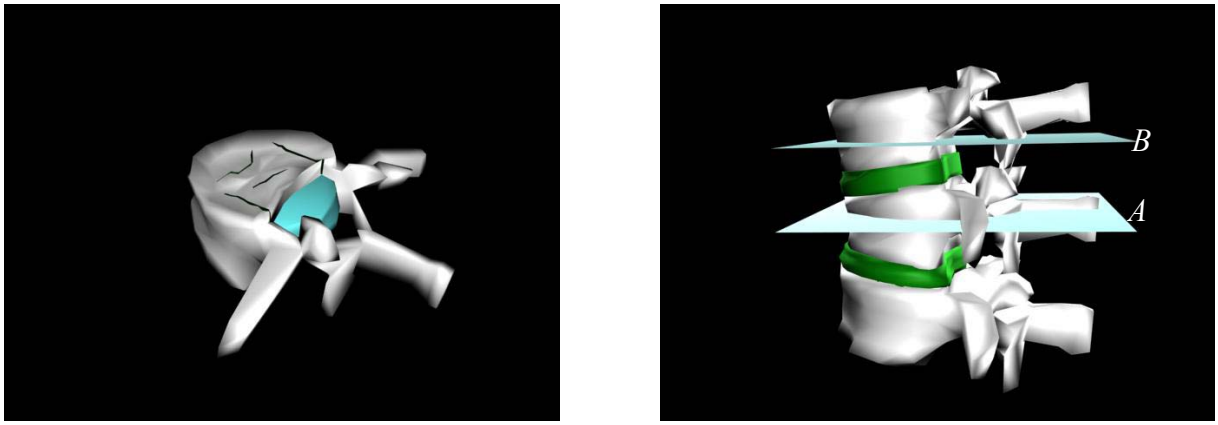

(A) (B)

Fig.1 Spatial relation of a fractured vertebral bone with neighboring normal vertebral bodies

△Gray area: bones. Green areas: disc spaces. Blue areas: bone fragment bursting to the canal. Black areas: cracks inside the body.

(A) A fractured vertebral bone in which the canal has a burst fragment at the canal and the body has cracks.

(B) A spine with a fractured bone. Transverse section *A* passes through the pedicle and lamina, while *B* does not.

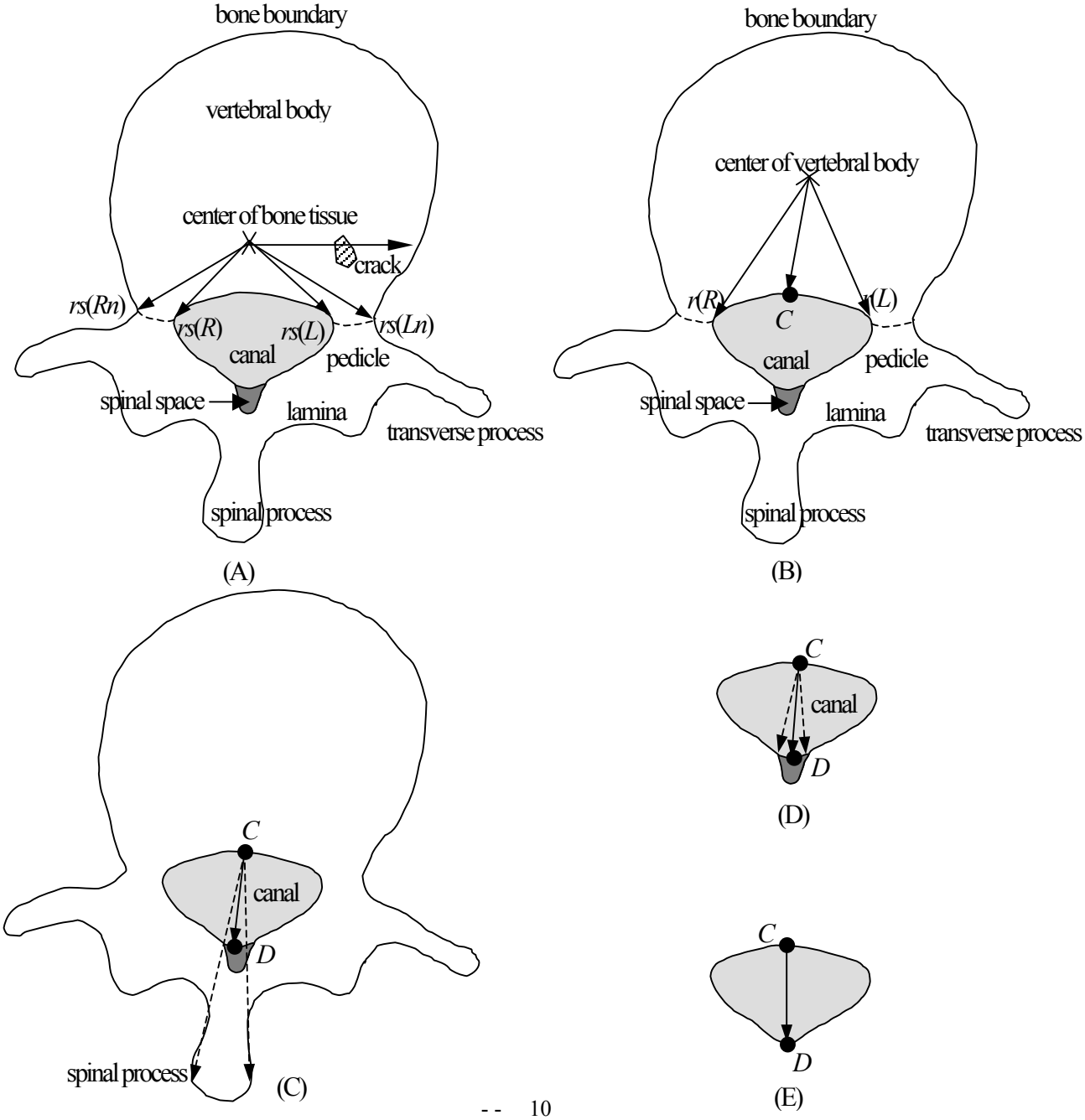

Fig.2 Image matching of bone boundary on a transverse section to obtain a B-spline approximate vertebral body.

(A) Determination of center of vertebral bone by averaging pixels of bone and disc substances. Determination of concave feature of the body enclosing the canal forming the canal by intersection computation.

(B) Determination of center and boundary of vertebral body by B-spline approximation

(C) Canal diameter determination by intersections of the vectors from the canal to spinal process

(D) Canal diameter determination by intersections of the vectors from the canal to spinal space

(E) Canal diameter determination by quadric approximation of the canal

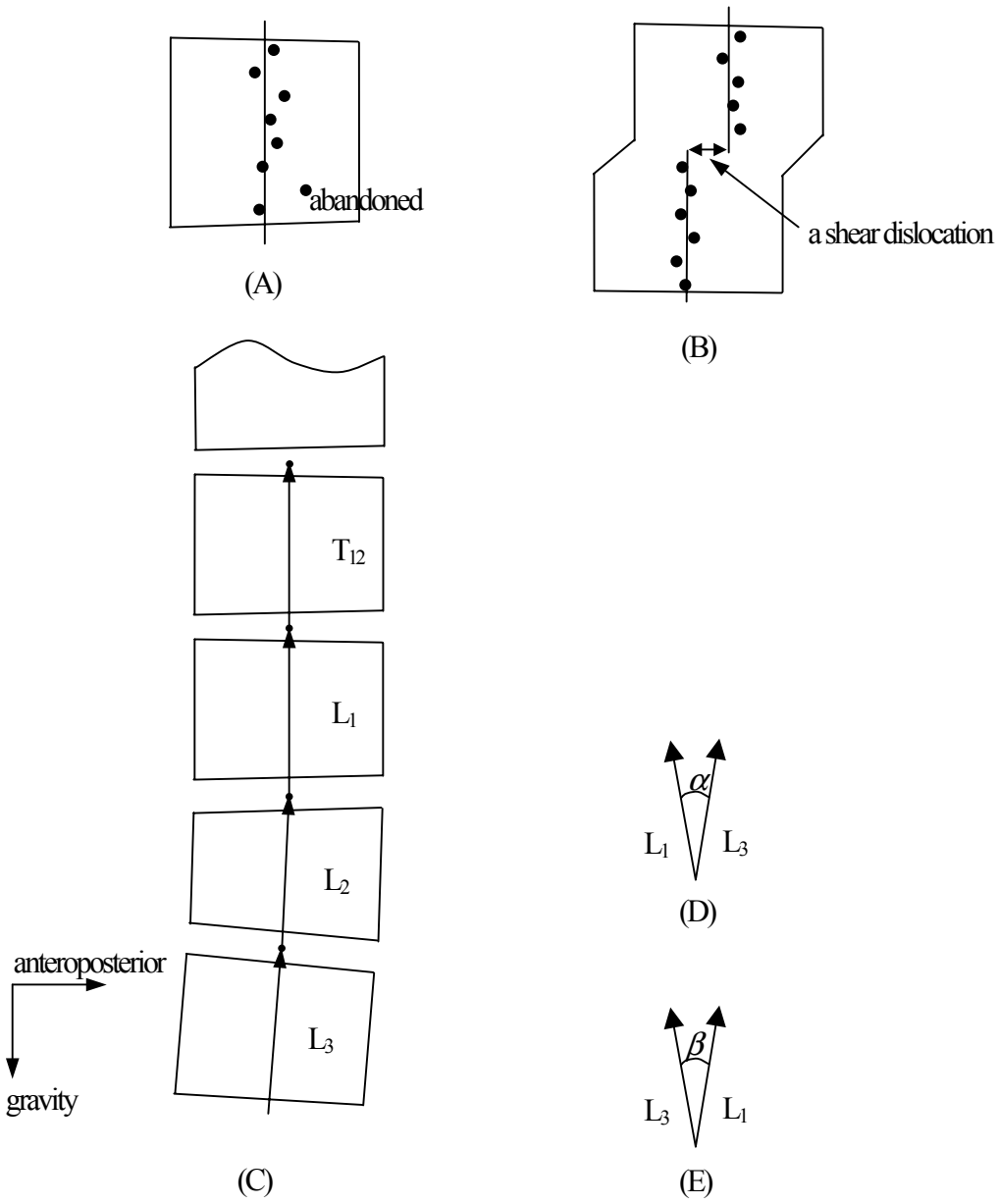

Fig.3 Determination of anatomic curve of a fractured spine

(A) Centerline of a vertebral body determined by regressing the centers on all sections passing the body

(B) Shear dislocation separated by two centerlines regressing two separate groups pf centers

(C) Centerlines of vertebral bodies representing the anatomic curve after the fracture

(D) Angle between the two centerlines of the above and below vertebral bodies of the fractured body.

(E) Normal angle of the above and below vertebral bodies, indicating the angle after recovery

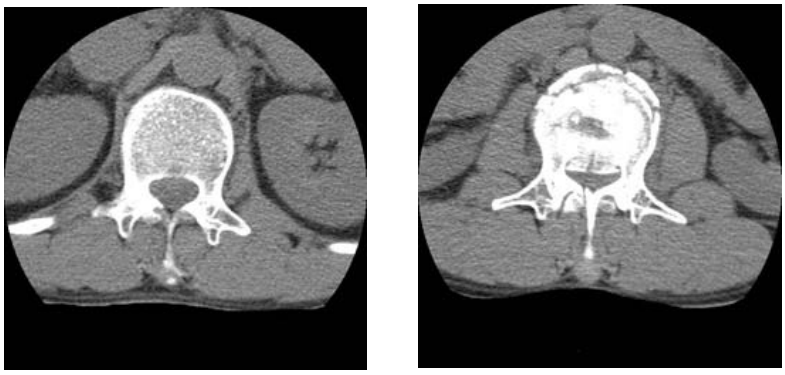

(A) (B)

Fig.4 CT transverse sections of vertebral bones

(A) A section passes L1 without fracture

(B) A section passes L2 with fracture

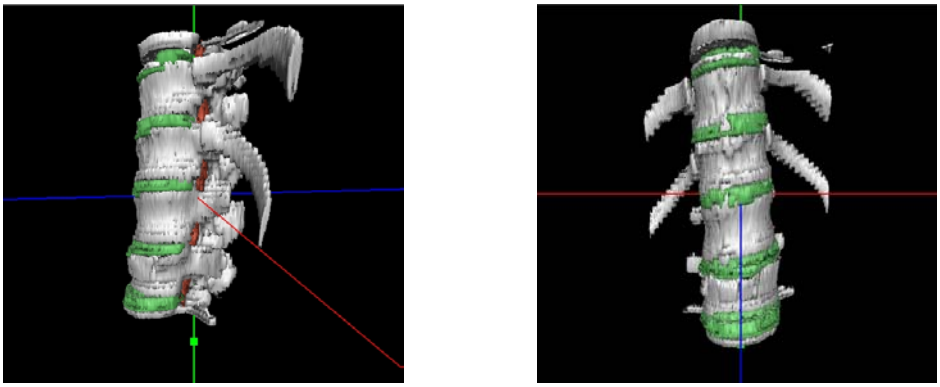

(A) (B)

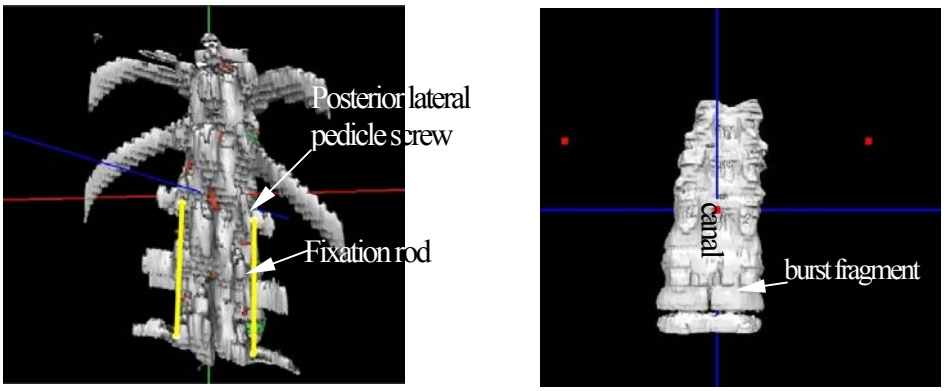

(C) (D)

Fig.5 3D image reconstructed from 48 CT transverse sections (without interpolations)

△Gray area: bones. Green areas: disc spaces. Red areas: spinal code or roots. Yellow area: posterior lateral pedicle screws and reduction fixation rods

(A) Lateral view: indicates compression on L2, especially the anterior column bringing kyphosis

(B) Frontal view: indicates un-symmetric horizontal compression on L2 bringing scoliosis

(C) Posterior view: indicates positions for inserting posterior lateral pedicle screws and reduction rods for fracture reduction and posterior fusion

(D) Posterior view: indicates burst fragment to the canal at L2 , onlyr recognized vertebral bodies were reconstructed

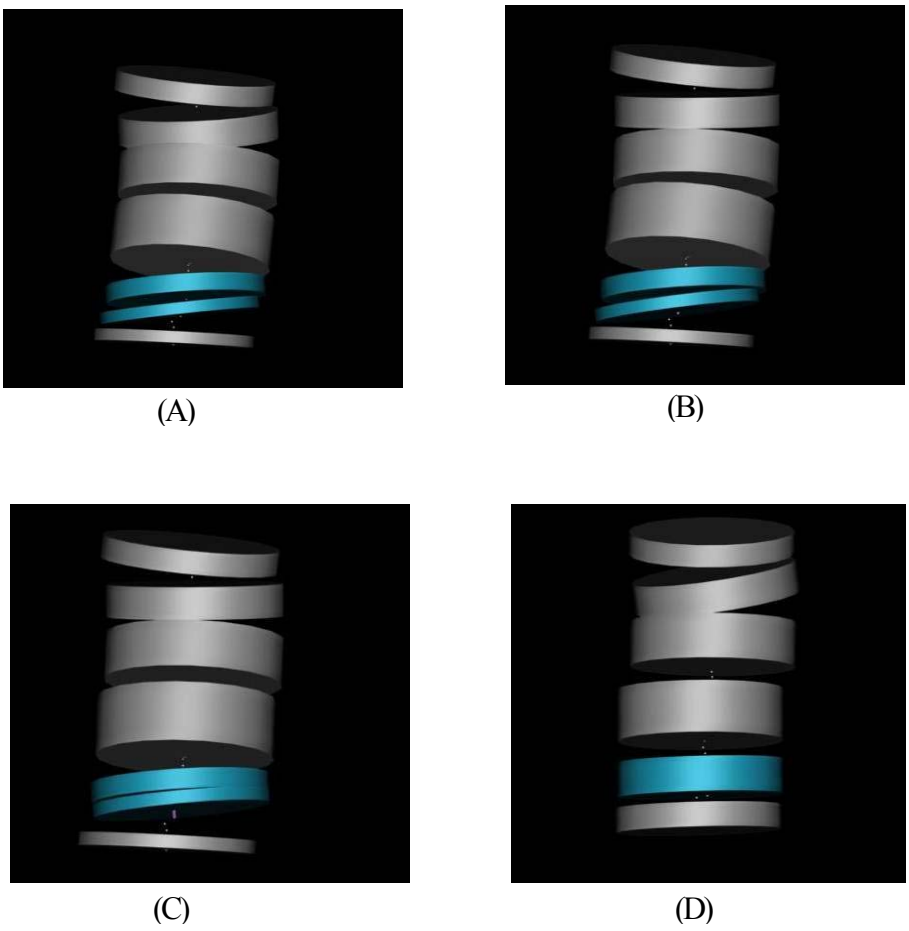

(A) (B)

(C) (D)

Fig.6 3D image abalysis for 48 CT transverse sections

△Gray area: bones. Green areas: disc spaces. Red areas: nerve code or roots.

(A) 3D simplified vertebral bodies with the fractured body L2

(B) Interpolation of the heights and angles between the fractured L2 and the assumed normal L2

(C) Interpolation of the heights and angles between the fractured L2 and the assumed normal L2

(D) 3D simplified vertebral bodies with the assumed normal L2 body wherein the height is interpolated by neighboring bodies and the angle inferred from the normal anatomic curve